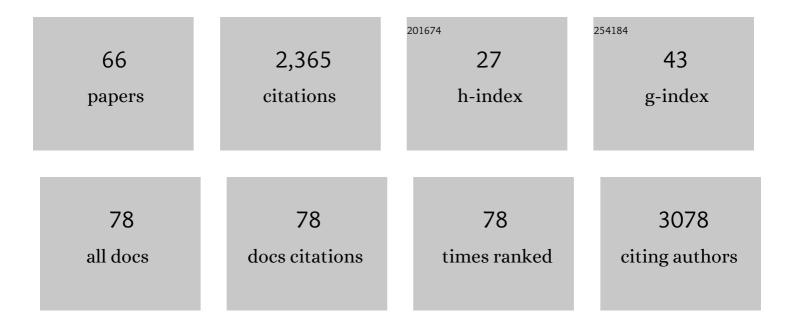
List of Publications by Year in descending order

Source: https://exaly.com/author-pdf/5765766/publications.pdf Version: 2024-02-01



#	Article	IF	CITATIONS
1	Measurement of atom resolvability in cryo-EM maps with Q-scores. Nature Methods, 2020, 17, 328-334.	19.0	230
2	A Single Immunization with Spike-Functionalized Ferritin Vaccines Elicits Neutralizing Antibody Responses against SARS-CoV-2 in Mice. ACS Central Science, 2021, 7, 183-199.	11.3	134
3	Accelerated cryo-EM-guided determination of three-dimensional RNA-only structures. Nature Methods, 2020, 17, 699-707.	19.0	119
4	Cryo-EM and antisense targeting of the 28-kDa frameshift stimulation element from the SARS-CoV-2 RNA genome. Nature Structural and Molecular Biology, 2021, 28, 747-754.	8.2	91
5	Cryo-EM structure of a 40ÂkDa SAM-IV riboswitch RNA at 3.7 à resolution. Nature Communications, 2019, 10, 5511.	12.8	90
6	Ultra-thermostable RNA nanoparticles for solubilizing and high-yield loading of paclitaxel for breast cancer therapy. Nature Communications, 2020, 11, 972.	12.8	86
7	MOF-derived core/shell C-TiO2/CoTiO3 type II heterojunction for efficient photocatalytic removal of antibiotics. Journal of Hazardous Materials, 2021, 406, 124675.	12.4	81
8	Magnetic Fe 3 O 4 nanoparticles induced effects on performance and microbial community of activated sludge from a sequencing batch reactor under long-term exposure. Bioresource Technology, 2017, 225, 377-385.	9.6	80
9	Automated Sequence Design of 3D Polyhedral Wireframe DNA Origami with Honeycomb Edges. ACS Nano, 2019, 13, 2083-2093.	14.6	77
10	Cryo-EM Structures of Human Drosha and DGCR8 in Complex with Primary MicroRNA. Molecular Cell, 2020, 78, 411-422.e4.	9.7	75
11	Resolving individualÂatoms of protein complex by cryo-electron microscopy. Cell Research, 2020, 30, 1136-1139.	12.0	69
12	Impact of sulfadiazine on performance and microbial community of a sequencing batch biofilm reactor treating synthetic mariculture wastewater. Bioresource Technology, 2017, 235, 122-130.	9.6	66
13	Impact of ampicillin on the nitrogen removal, microbial community and enzymatic activity of activated sludge. Bioresource Technology, 2019, 272, 337-345.	9.6	61
14	Cryo-EM structures of full-length Tetrahymena ribozyme at 3.1ÂÃ resolution. Nature, 2021, 596, 603-607.	27.8	59
15	Long-term impacts of titanium dioxide nanoparticles (TiO 2 NPs) on performance and microbial community of activated sludge. Bioresource Technology, 2017, 238, 361-368.	9.6	55
16	Biodegradation of hydrolyzed polyacrylamide by the combined expanded granular sludge bed reactor-aerobic biofilm reactor biosystem and key microorganisms involved in this bioprocess. Bioresource Technology, 2018, 263, 153-162.	9.6	54
17	Rapid prototyping of arbitrary 2D and 3D wireframe DNA origami. Nucleic Acids Research, 2021, 49, 10265-10274.	14.5	51
18	Low-Temperature and Solution-Processable Zinc Oxide Transistors for Transparent Electronics. ACS Omega, 2017, 2, 8990-8996.	3.5	50

#	Article	IF	CITATIONS
19	Gambogenic acid induces ferroptosis in melanoma cells undergoing epithelial-to-mesenchymal transition. Toxicology and Applied Pharmacology, 2020, 401, 115110.	2.8	47
20	Highly sensitive solution-gated graphene transistors for label-free DNA detection. Biosensors and Bioelectronics, 2019, 136, 91-96.	10.1	45
21	Terahertz polarization splitter based on orthogonal microstructure dual-core photonic crystal fiber. Applied Optics, 2013, 52, 3305.	1.8	41
22	Insights into the effect of nickel (Ni(II)) on the performance, microbial enzymatic activity and extracellular polymeric substances of activated sludge. Environmental Pollution, 2019, 251, 81-89.	7.5	41
23	Mapping the catalytic conformations of an assembly-line polyketide synthase module. Science, 2021, 374, 729-734.	12.6	41
24	Coupling of ssRNA cleavage with DNase activity in type III-A CRISPR-Csm revealed by cryo-EM and biochemistry. Cell Research, 2019, 29, 305-312.	12.0	40
25	Slit2 Promotes Angiogenic Activity Via the Robo1-VEGFR2-ERK1/2 Pathway in Both In Vivo and In Vitro Studies. , 2015, 56, 5210.		38
26	Inhibition mechanisms of AcrF9, AcrF8, and AcrF6 against type I-F CRISPR–Cas complex revealed by cryo-EM. Proceedings of the National Academy of Sciences of the United States of America, 2020, 117, 7176-7182.	7.1	35
27	Cryo-EM structures of <i>Helicobacter pylori</i> vacuolating cytotoxin A oligomeric assemblies at near-atomic resolution. Proceedings of the National Academy of Sciences of the United States of America, 2019, 116, 6800-6805.	7.1	33
28	Hydrolyzed polyacrylamide-containing wastewater treatment using ozone reactor-upflow anaerobic sludge blanket reactor-aerobic biofilm reactor multistage treatment system. Environmental Pollution, 2021, 269, 116111.	7.5	30
29	Model-Driven Redox Pathway Manipulation for Improved Isobutanol Production in Bacillus subtilis Complemented with Experimental Validation and Metabolic Profiling Analysis. PLoS ONE, 2014, 9, e93815.	2.5	28
30	Long-term effect of different Cu(II) concentrations on the performance, microbial enzymatic activity and microbial community of sequencing batch reactor. Environmental Pollution, 2019, 255, 113216.	7.5	26
31	Physiological role of the novel salicylaldehyde dehydrogenase NahV in mineralization of naphthalene by Pseudomonas putida ND6. Microbiological Research, 2011, 166, 643-653.	5.3	25
32	One-step scalable synthesis of honeycomb-like g-C <sub>3</sub> N <sub>4</sub> with broad sub-bandgap absorption for superior visible-light-driven photocatalytic hydrogen evolution. RSC Advances, 2019, 9, 32674-32682.	3.6	20
33	Impacts of silver nanoparticles on performance and microbial community and enzymatic activity of a sequencing batch reactor. Journal of Environmental Management, 2017, 204, 667-673.	7.8	19
34	Structure of the G protein chaperone and guanine nucleotide exchange factor Ric-8A bound to Gαi1. Nature Communications, 2020, 11, 1077.	12.8	18
35	Tailoring aromatic ring-terminated edges of g-C <sub>3</sub> N <sub>4</sub> nanosheets for efficient photocatalytic hydrogen evolution with simultaneous antibiotic removal. Catalysis Science and Technology, 2020, 10, 5470-5479.	4.1	16
36	In Vivo Study of Retinal Transmission Function in Different Sections of the Choroidal Structure Using Multispectral Imaging. , 2015, 56, 3731.		15

#	Article	IF	CITATIONS
37	Effect of magnesium oxide nanoparticles on microbial diversity and removal performance of sequencing batch reactor. Journal of Environmental Management, 2018, 222, 475-482.	7.8	13
38	Single and combined effects of divalent copper and hexavalent chromium on the performance, microbial community and enzymatic activity of sequencing batch reactor. Science of the Total Environment, 2020, 719, 137289.	8.0	13
39	Molecular basis for ATPase-powered substrate translocation by the Lon AAA+ protease. Journal of Biological Chemistry, 2021, 297, 101239.	3.4	12
40	Insights into the effects of single and combined divalent copper and humic acid on the performance, microbial community and enzymatic activity of activated sludge from sequencing batch reactor. Chemosphere, 2020, 249, 126165.	8.2	11
41	p53-mediated ferroptosis is required for 1-methyl-4-phenylpyridinium-induced senescence of PC12 cells. Toxicology in Vitro, 2021, 73, 105146.	2.4	11
42	Dual-Porous Fiber-Based Low Loss Broadband Terahertz Polarization Splitter. IEEE Photonics Technology Letters, 2014, 26, 1399-1402.	2.5	10
43	Insights into long-term effects of amino-functionalized multi-walled carbon nanotubes (MWCNTs-NH2) on the performance, enzymatic activity and microbial community of sequencing batch reactor. Environmental Pollution, 2019, 254, 113118.	7.5	10
44	A 3.4-Ã cryo-electron microscopy structure of the human coronavirus spike trimer computationally derived from vitrified NL63 virus particles. QRB Discovery, 2020, 1, e11.	1.6	10
45	Planar 2D wireframe DNA origami. Science Advances, 2022, 8, .	10.3	10
46	Performance evaluation and microbial community shift of a sequencing batch reactor under silica nanoparticles stress. Bioresource Technology, 2017, 245, 673-680.	9.6	9
47	A cluster of atypical resistance genes in soybean confers broad-spectrum antiviral activity. Plant Physiology, 2022, 188, 1277-1293.	4.8	9
48	Processive cleavage of substrate at individual proteolytic active sites of the Lon protease complex. Science Advances, 2021, 7, eabj9537.	10.3	9
49	A prototype protein nanocage minimized from carboxysomes with gated oxygen permeability. Proceedings of the National Academy of Sciences of the United States of America, 2022, 119, .	7.1	9
50	Effects of transient 3-chloroaniline shock loading on the performance, microbial community and enzymatic activity of sequencing batch reactor. Journal of Environmental Management, 2020, 258, 110017.	7.8	8
51	Constructing a Pt/YMn <sub>2</sub> O <sub>5</sub> Interface to Form Multiple Active Centers to Improve the Hydrothermal Stability of NO Oxidation. ACS Applied Materials & Interfaces, 2022, 14, 20875-20887.	8.0	8
52	Complete three-dimensional structures of the Lon protease translocating a protein substrate. Science Advances, 2021, 7, eabj7835.	10.3	7
53	Cryo-EM, Protein Engineering, and Simulation Enable the Development of Peptide Therapeutics against Acute Myeloid Leukemia. ACS Central Science, 2022, 8, 214-222.	11.3	7
54	Novel Fe <sub>2</sub> O <sub>3</sub> /PZT Nanorods for Ferroelectric Polarization-Enhanced Photoelectrochemical Water Splitting. Energy & Fuels, 2020, 34, 16927-16935.	5.1	6

#	Article	IF	CITATIONS
55	Bacteriophage Twort protein Gp168 is a β-clamp inhibitor by occupying the DNA sliding channel. Nucleic Acids Research, 2021, 49, 11367-11378.	14.5	6
56	Fiber Bragg Gratings Based Cyclic Strain Measuring of Weld Toes of Cruciform Joints. Applied Sciences (Switzerland), 2019, 9, 2939.	2.5	5
57	Long-term impacts of carboxyl functionalized multi-walled carbon nanotubes on the performance, microbial enzymatic activity and microbial community of sequencing batch reactor. Bioresource Technology, 2019, 286, 121382.	9.6	5
58	3D RNA nanocage for encapsulation and shielding of hydrophobic biomolecules to improve the in vivo biodistribution. Nano Research, 2020, 13, 3241-3247.	10.4	4
59	Bacteriophage protein PEIP is a potent Bacillus subtilis enolase inhibitor. Cell Reports, 2022, 40, 111026.	6.4	4
60	Analysis of the Fatigue Crack Evolution of Corrugated Web Girders. Metals, 2019, 9, 869.	2.3	3
61	Effects of aluminum oxide nanoparticles on the performance, extracellular polymeric substances, microbial community and enzymatic activity of sequencing batch reactor. Environmental Technology (United Kingdom), 2021, 42, 366-376.	2.2	3
62	Performance of a sequential anaerobic baffled reactor (ABR)/membrane bioreactor (MBR) system treating caffeine wastewater. , 2011, , .		1
63	Evolution of microstructure and properties of Ag and Si-doped AlMg alloys. Journal of Materials Science: Materials in Electronics, 2021, 32, 16889-16899.	2.2	1
64	Development of fast LLR algorithms to retrieve atmospheric profiles from IRAS/FY3B infrared measurements. , 2016, , .		0
65	Land surface temperature retrieval from Landsat-8 data. , 2017, , .		0
66	Molecular Characterization of Polar Compounds in Crude Oil Affecting Sandstone Wettability Revealed by Fourier Transform-Ion Cyclotron Resonance-Mass Spectrometry. SPE Journal, 2022, , 1-14.	3.1	0